Fuel Processing Technology 245 (2023) 107745

Contents lists available at ScienceDirect

Fuel Processing Technology

journal homepage: www.elsevier.com/locate/fuproc

Boosting the activity in the direct conversion of CO_2/CO mixtures into gasoline using ZnO-ZrO_2 catalyst in tandem with HZSM-5 zeolite

Onintze Parra, Ander Portillo, Javier Ereña, Andrés T. Aguayo, Javier Bilbao, Ainara Ateka *

Department of Chemical Engineering, University of the Basque Country UPV/EHU, P.O. Box 644, 48080 Bilbao, Spain

ARTICLE INFO

Keywords:
CO_2 hydrogenation
HZSM-5 zeolite
Methanol synthesis
Gasoline synthesis
Isoparaffinic gasoline
Catalyst

ABSTRACT

The direct production of C_{5+} hydrocarbons from CO_2/CO mixtures with methanol as intermediate is an attractive alternative for the production of gasoline from CO_2 and syngas derived from biomass. With this purpose, the performance of CuO-ZnO-ZrO_2 (CZZ), In_2O_3-ZrO_2 (IZ) and ZnO-ZrO_2 (ZZ) metallic oxides was compared by using them in tandem with a HZSM-5 zeolite. The catalysts were analyzed by means of N_2 adsorption-desorption, XRD, XRF, H_2-TPR and NH_3-TPD. Two series of runs were performed in a packed bed reactor: (i) the methanol synthesis with the metallic oxides as catalysts, at 250–430 °C; 50 bar; CO_2/CO_x, 0–1; H_2/CO_x, 3; space time 6 g_{cat} h mol_C^{-1}; and (ii) the synthesis of hydrocarbons with the tandem catalysts with a metallic oxide/zeolite mass ratio of 1/1, at 340, 380 and 420 °C; 30 and 50 bar; CO_2/CO_x, 0.5 and 1; H_2/CO_x, 3; space time 12 g_{cat} h mol_C^{-1}. The results were quantified in terms of yield and selectivity of the product fractions and CO_2 and CO_x (CO_2 + CO) conversion. The higher methanol yield attained with the CZZ catalyst for the CO + H_2 feed and its mixing with CO_2 was faded by the problem of its sintering above 350 °C (minimum temperature required for the extent of methanol conversion to hydrocarbons). The IZ and ZZ catalysts were active, selective to methanol and stable both in the methanol synthesis and when used in IZ/HZSM-5 and ZZ/HZSM-5 tandem catalysts. Excellent results were obtained with the latter, which resulted in a 20.7% yield of C_{5+} hydrocarbon fraction at 420 °C and 50 bar, with CO_2 and CO_x conversion of 39.7% and 28.4%, respectively. This fraction corresponded to isoparaffinic gasoline, with isoparaffin yield (mainly C_5 and C_6) surpassing 20% and low concentration of aromatics (0.1%) that led to a Research Octane Number of 91.8. This composition results attractive for its integration into the refineries gasoline pool. Furthermore, the changes of the CO_2/CO_x ratio in the feed barely affected the yield and composition of the gasoline obtained with the ZZ/HZSM-5 catalyst, stating its great versatility.

1. Introduction

The rising CO_2 emissions, global warming and the risks posed by climate change have put the carbon dioxide capture and utilization (CCU) technologies in the limelight. In this scenario, the catalytic processes, especially the catalytic hydrogenation of CO_2 for the production of liquid fuels and bulk chemicals, receive a great deal of attention [1–4]. The interest of these processes leads in their contribution to the circular carbon economy, by replacing the fossil sources by CO_2 as carbon source, and using green hydrogen and renewable energy for the products with an increasing demand in the petrochemical industry [5].

The processes for the direct synthesis of hydrocarbons from CO_2 (in a single reactor) show several thermodynamic benefits as opposed to the indirect routes (in two stages). Moreover, lower capital investment and operating cost are required. Two main routes can be distinguished for the direct conversion of CO_2 into hydrocarbons, and both of them are carried out by means of tandem catalysts [6–9]. In the Modified Fischer Tropsch (MFT) synthesis, CO_2 reacts according to the Anderson-Schulz-Flory (ASF) mechanism, characteristic of the FT synthesis, using Fe- or Co-based catalysts. The products are in situ reformed over a zeotype providing the adequate acidity and shape selectivity to the selective production of the desired hydrocarbon fraction [10,11]. On the other hand, in the route with oxygenates (methanol/dimethyl ether (DME)) as intermediates, OX/ZEO (metallic oxide/zeotype) catalysts are employed, in which the metallic oxide is the responsible of the formation of the oxygenates, and the zeotype is used for the selective conversion of these into hydrocarbons [12,13]. In both routes, the integration of the two reaction stages helps to: (i) diminish the required investment and the operating costs in contrast to the processes with two reactors; and (ii) to benefit the thermodynamics, because of the shifting of the

* Corresponding author.
E-mail address: ainara.ateka@ehu.eus (A. Ateka).

https://doi.org/10.1016/j.fuproc.2023.107745
Received 30 January 2023; Received in revised form 8 March 2023; Accepted 14 March 2023
Available online 22 March 2023

equilibrium of the CO_2 conversion step. Guo et al. [14] made a comprehensive thermodynamic study of the hydrogenation of CO_2 to alcohols and hydrocarbons (ethylene, propylene, benzene), proving the thermodynamic feasibility of these processes and pointing out thermodynamics as the necessary preliminary step to establish the appropriate reaction conditions and catalyst to maximize CO_2 conversion and hydrocarbon yield.

The knowledge on the catalysts and mechanisms of the routes for the direct conversion of CO_2 into hydrocarbons is based on the prior knowledge of the individual stages in the indirect routes. In that way, for methanol/DME synthesis, Cu-based metallic catalysts (mainly Cu-ZnO-Al_2O_3) have been used in the industry (originally with syngas and more recently for CO_2 hydrogenation), due to their low cost and high performance [15–17]. The role of the ZnO is key to increase the dispersion of Cu and to minimize its sintering [15,18]. The presence of Al_2O_3 as promoter provides surface area and eases the separation of Cu-ZnO sites, resulting in an increase of the stability as well as mechanical resistance [19]. The replacement of Al_2O_3 by ZrO_2 forming Cu-ZnO-ZrO_2 catalysts resulted to improve the stability of the catalyst, which is especially interesting in the CO_2 hydrogenation due to the high content of H_2O in the medium [20,21]. The hydrogenation of CO_2 to methanol over Cu-based catalysts is considered to proceed according to the formate species (HCOO*) as first intermediate species and successive hydrogenations [22–24]: $CO_2 \rightarrow HCOO^* \rightarrow HCOOH^* \rightarrow H_2COOH^* \rightarrow H_2CO^* \rightarrow H_3CO^* \rightarrow CH_3OH^* \rightarrow CH_3OH$. The smallest extent of the alternative route, i.e., the conversion of CO_2 into CO by means of the reverse Water Gas Shift (rWGS) reaction and the hydrogenation of CO to formyl species, is explained by the instability of this intermediate, that is decomposed to form CO and H_2.

Among the catalysts developed to avoid the limitations (temperature, H_2O concentration) of Cu-based catalysts in the direct synthesis of hydrocarbons from CO_2, those based on In_2O_3 have received great attention due to their high activity for the conversion of CO_2 into methanol and their stability at the temperature required (>350 °C) for the conversion of methanol/DME to hydrocarbons [6,25,26]. Moreover, In_2O_3 is known to suppress the rWGS reaction, avoiding the initial CO_2 to CO shift taking place over the Cu-based catalysts [27]. In In_2O_3 catalysts, CO_2 is adsorbed and activated in the oxygen vacancies, and produces formate species following the sequence [28,29]: $CO_2 \rightarrow HCOO^* \rightarrow HCOOH^* \rightarrow H_2COOH^* \rightarrow H_2COHOH^* \rightarrow H_2CO^* \rightarrow H_3CO^* \rightarrow CH_3OH^* \rightarrow CH_3OH$. The incorporation of ZrO_2 as promoter boosts the formation of additional oxygen vacancies and increases the stability of In_2O_3 [27,30,31]. The properties of In_2O_3-ZrO_2 have been improved by incorporating Ni [32] and noble metals such as Pd [33,34], Rh [35], Pt [36] or Au [37].

Zn containing oxides have also pointed out among methanol synthesis catalysts by providing high CO_2 conversion and methanol selectivity, especially when combined with ZrO_2 as support, which helps to increase methanol selectivity [38,39]. The properties of ZnO-ZrO_2 catalysts are enhanced with the incorporation of noble metals [40]. Wang et al. [41] established that the reaction mechanism of CO_2 hydrogenation to methanol over ZnO-ZrO_2 based catalyst are both formate and CO reaction pathway. In addition to the great performance, this catalyst has shown to be highly stable, due to the formation of the $ZrZnO_x$ solid solution, and it does not undergo deactivation in long catalytic runs (up to 500 h).

As aforementioned, in the direct synthesis of hydrocarbons from CO_2, for the methanol/DME conversion into hydrocarbons (second reaction stage), zeolite-based catalysts are used. The activity, selectivity and stability of the zeolites are a direct consequence of their properties, especially of the shape selectivity and the acidity [42]. It is well established the dual cycle mechanism for the conversion of methanol/DME [43,44]. This mechanism takes place by the formation of light olefins as primary products by means of the cycles of alkylation/dealkylation of the intermediate polymethylbenzenes confined in the catalysts, and of oligomerization/cracking of the light olefins. The extent of the secondary reactions (alkylation, isomerization, condensation to aromatics) favors the formation of light paraffins (by hydrogen transfer and cracking), BTX aromatics and not aromatic C_{5+} hydrocarbons, especially interesting for their use as green gasoline. Therefore, the main challenge is the election of a selective catalyst for each aim. For the selective production of light olefins, SAPO-34 (CHA framework) is highly employed [42,45–47]. As an example of good results in the literature, Zhang et al. obtained with Ga_mCrO_x/HSAPO-34 catalyst a CO_2 conversion of 11.9% and a selectivity of light olefins of 87.3% (excluding CO) at 350 °C and a selectivity of 34.5% to CO, at 350 °C and 30 bar [48]. On the other hand, the drawback of the rapid deactivation by coke deposition (assisted by the easy confinement of the polymethylbenzenes in the cages of the porous structure of SAPO-34) is lessened with the particular operating conditions (high H_2 and H_2O partial pressure) [49].

HZSM-5 zeolite is the most studied catalyst for the production of higher hydrocarbons (such as aromatics or linear paraffins in the gasoline-range) from CO_2 [13,50,51], owing to its MFI structure, that eases a major extent of the dual cycle mechanism in the conversion of methanol/DME and also of some of the secondary reactions. Moreover, its versatility towards different products in the conversion of methanol/DME by the generation of hierarchical porous structures, the adjustment of the acidity and the incorporation of metals is well established [52–54]. The porous structure of HZSM-5 zeolite (without cages in the intersections) facilitates the diffusion of the intermediate coke precursors, delaying their confinement and attenuating the deactivation [55]. Ticali et al. [50] related the higher interest of $ZnZrO_2$/HZSM-5 catalyst for the production of aliphatic compounds in contrast to $ZnZrO_2$/SAPO-34 highlighting higher conversion and stability of HZSM-5 at lower temperature and space time.

After the development of the direct synthesis of hydrocarbons from syngas, the direct conversion of hybrid feeds (H_2/CO_2/CO) is gaining awareness [46,56], on account of the interest in terms of sustainability and joint valorization of CO_2 with syngas obtained from biomass [57,58] or waste [59,60]. Moreover, syngas co-feeding partially provides the required hydrogen. Additionally, CO co-feeding also favors thermodynamically the production of methanol as compared to the hydrogenation of CO_2 by attenuating the extent of the reverse Water Gas Shift reaction [14,61]. Moreover, the differences in the role of CO when it is formed by the rWGS reaction as a byproduct or when it is co-fed with CO_2 has been assessed [14].

In this context, the performance of three different metallic oxides (CuO-ZnO-ZrO_2, In_2O_3-ZrO_2, ZnO-ZrO_2) was compared for their interest to activate the methanol synthesis step in the direct production of gasoline-range C_{5+} hydrocarbons from CO_2 and mixtures of CO_2/CO. The results with these catalysts in the synthesis of methanol are continued in this manuscript with those obtained using them in tandem together with HZSM-5 zeolite, aiming at selecting both the metallic oxide and the appropriate operating conditions for the selective production of isoparaffinic gasoline with commercial interest as a fuel. The results allow to assess the prospects of a ZnO-ZrO_2/HZSM-5 catalyst for an attractive target (gasoline production), that has received less attention in the literature, and which is complementary to other goals in the catalytic CO_2 valorization processes, such as the production of light olefins or aromatics. Considering the importance of the results for the decarbonization objective, attention will also be paid to the CO_2 and CO_x conversion results, attending to the interest of also valorizing the syngas obtained from biomass or wastes.

2. Experimental section

2.1. Preparation of the catalysts

The metallic catalysts for the methanol synthesis step, i.e., CuO-ZnO-ZrO_2, In_2O_3-ZrO_2 and ZnO-ZrO_2, named in a simplified way CZZ, IZ and ZZ, respectively, were synthesized following a co-precipitation method. CZZ catalyst was prepared with a Cu/Zn/Zr atomic ratio of 2/1/1 following the method described by Sánchez-Contador et al. [20]. IZ catalyst, with an atomic In/Zr ratio of 2/1, was prepared following the

method described by Portillo et al. [30]. For the synthesis of ZZ, a metal nitrate solution with 6.00 g of $Zn(NO_3)_2{\cdot}6H_2O$ (Sigma-Aldrich) and 13.69 g of $ZrO(NO_3)_2{\cdot}6H_2O$ (Sigma-Aldrich) was co-precipitated over 59.12 mL of deionized water, and a $(NH_4)_2CO_3$ solution (VWR Chemicals, 1 M) was added dropwise under continuous stirring to form a precipitate with an atomic Zn/Zr ratio of 1/2.5. This synthesis method was based on a previous work of Li et al. [62] and slight modifications were considered. The three catalysts were prepared at 70 °C and neutral pH. After the co-precipitation, the catalysts were aged, filtered and washed with deionized water. Afterwards, the catalysts were dried and calcined (at 300 °C for 10 h, at 500 °C for 1 h and at 500 °C for 5 h for CZZ, IZ and ZZ catalysts, respectively) in order to provide the corresponding metal oxides, according to the protocols established for each catalyst [20,30,62]. The resulting powders were pelletized to provide higher mechanical resistance, and sieved to a particle size in the 125–250 μm range.

As acid catalyst, a commercial HZSM-5 zeolite (Zeolyst International) with a Si/Al ratio of 140 was used. The election of the zeolite is a complex decision. This Si/Al ratio was selected to minimize cracking reactions and to increase the gasoline yield. The zeolite, provided in ammonium form was calcined at 575 °C for 2 h to obtain the acid form, pelletized and sieved to a particle size between 300 and 400 μm. These calcination temperature is appropriate for equilibrating the catalyst, so that it can recover its activity when used in reaction-regeneration cycles, after the elimination of the coke by air combustion at 550 °C [63]. The different particle size of both catalysts was selected as to ensure the easy separation after the reaction, having formerly proved that no diffusional limitations occur with these sizes. The tandem catalysts (CZZ/HZSM-5, IZ/HZSM-5 and ZZ/HZSM-5) were prepared by physical mixture of both metallic and acid catalysts, with a metal/acid mass ratio of 1/1.

2.2. Characterization of the catalysts

The physical properties of the catalysts (Table 1) were determined by N_2 adsorption-desorption isotherms (Micromeritics ASAP 2010). For this, the samples were degassed in vacuum conditions prior to the analysis, in order to remove impurities and H_2O adsorbed on the surface of the catalyst. Afterwards, N_2 adsorption-desorption equilibrium stages were conducted at −196 °C. It is remarkable that among the metallic catalysts, CZZ has a more favorable porous structure for the access of the reactants and diffusion of the intermediates and products, with higher values of BET surface area (S_{BET}), pore volume and mean size of pore diameter, whereas the ZZ catalyst has the lowest values of these properties. The properties of the HZSM-5 catalyst are characteristic of this zeolite, and correspond to a mostly microporous structure, whereas the presence of mesopores is due to the pelletization step. It should be noted that the kinetic results in Section 3.2 highlight the minor importance of these properties and the fundamental role of the different activity of the active sites of the catalysts in the corresponding reaction mechanism.

The chemical composition and atomic ratios were quantified by X-Ray fluorescence (XRF), by means of a PANalytical wavelength dispersive X-ray fluorescence sequential spectrometer (WDXRF), model AXIOS, equipped with a Rh tube and three detectors (gas flow, scintillation and Xe sealing). Results are shown in Table S1. The structure was determined by X-Ray diffraction (XRD) with a PANalytical Xpert PRO diffractometer, equipped with copper tube ($\lambda Cu_{K\alpha} = 1.5418$ Å), a vertical goniometer (Bragg-Brentano geometry), secondary monochromator and PixCel detector. The measurement conditions were 40 kV/40 mA and the pattern was recorded in a $5 < 2\theta < 60$ range for CZZ catalyst and in a $5 < 2\theta < 80$ range for IZ and ZZ catalysts.

Table 1
Physical properties of the metallic and acid catalysts.

Catalyst	S_{BET} ($m^2\ g^{-1}$)	V_{micro} ($cm^3\ g^{-1}$)	V_p ($cm^3\ g^{-1}$)	d_p (nm)
CZZ	115	0.0028	0.25	10.2
IZ	80	0.0029	0.13	8.3
ZZ	48	0.0017	0.08	5.8
HZSM-5	414	0.0960	0.22	3.2

The normalized XRD patterns of the three metallic catalysts are gathered in Fig. 1. According to the diffractograms, IZ comprises cubic structure for both In_2O_3 and ZrO_2 oxides (in accordance with ICDD (International Center for Diffractional Data) #71–2195 and #49–1642, respectively), corresponding to the state with the highest catalytic activity [64]. On the other hand, hexagonal ZnO (in accordance with ICDD #36–1451) and cubic ZrO_2 (in accordance with ICDD #49–1642) structures were found in ZZ catalyst. Regarding the traditional CZZ catalyst, its structure was described thoroughly elsewhere [20]. Briefly, the characteristic peaks of CuO and ZnO oxides were visible on the spectra, while ZrO_2 peaks were not noticeable due to the high dispersion and small size of the crystals.

H_2 temperature programmed reduction (H_2-TPR) analyses were carried out (Micromeritics Autochem 2920) to study the reducibility of the catalysts. For this assay, 100 mg of sample were treated previous to the reduction by sweeping with He, to remove possible impurities and H_2O. The H_2-TPR analysis was carried out heating the sample up to 800 °C at a 2 °C min^{-1} rate in a diluted H_2 stream (10% H_2 in Ar). Attending to the TPR profiles (Fig. S1), CZZ is completely reduced at temperatures above 200 °C, whereas IZ and ZZ require higher temperature, so they might be in their oxide form at the beginning of the reactions. The same equipment was used for measuring the acidity by means of NH_3-TPD analyses. 50 μL min^{-1} NH_3 were injected at 150 °C until the saturation of the sample. The desorption step was conducted with a 5 °C min^{-1} rate up to 550 °C in a He stream. Fig. S2 exhibits the NH_3-TPD profile of the HZSM-5 catalyst. The total acidity of this zeolite accounts for 62 $\mu mol_{NH3}\ g_{cat}^{-1}$, with a peak at 190 °C and a higher one at 320 °C, stating low total acidity but a great presence of strong acid sites according to the classification in the literature [65].

2.3. Reaction and analysis equipment

The catalytic runs were performed in an isothermal packed bed reactor (PID Eng & Tech Microactivity Reference). The reactor is made of 316 stainless steel and has a ceramic coating to avoid the contact of the reactants with the steel and so, any possible side reaction. The

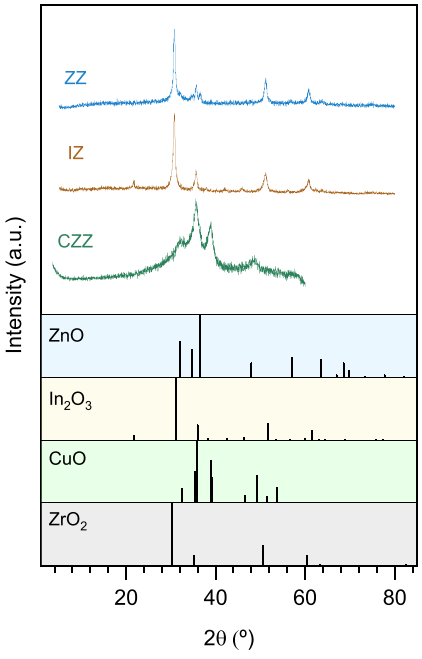

Fig. 1. XRD patterns of the metallic catalysts.

internal diameter of the reactor is of 9 mm and it has an effective length of 10 cm. This equipment can operate at a pressure up to 100 bar and temperatures up to 700 °C. The catalytic bed is composed of a mixture of the catalyst and an inert solid (SiC), in order to ensure isothermal conditions of the bed, to avoid preferential flow paths and to achieve sufficient bed height when operating at low space time values.

The feed and reaction product streams were analyzed on-line in a micro chromatograph (Varian CP-4900, Agilent), equipped with three analysis modules composed of TCD detectors and the following columns: (i) molecular sieve (MS-5) (10 m × 12 μm) for the quantification of H_2, O_2, N_2 and CO; (ii) Porapak Q (PPQ) (10 m × 20 μm) for the quantification of CO_2, methane, H_2O, C_2-C_4 hydrocarbons, methanol and DME; and (iii) 5 CB (CPSiL) (8 m × 2 μm) for the quantification of C_{5+} hydrocarbons.

The reaction runs of methanol synthesis (with the CZZ, IZ and ZZ metallic catalysts) were carried out under the following conditions: 250–430 °C; 50 bar; space time, 6 g_{cat} h mol_C^{-1}; CO_2/CO_x molar ratio in the feed, 0, 0.5 and 1; H_2/CO_x molar ratio in the feed, 3. The reactions for the direct synthesis of hydrocarbons (with the CZZ/HZSM-5, IZ/HZSM-5 and ZZ/HZSM-5 tandem catalysts) were performed under the following conditions: 340, 380 and 420 °C; 30 and 50 bar; space time, 12 g_{cat} h mol_C^{-1}; CO_2/CO_x ratio in the feed, 0.5 and 1; H_2/CO_x ratio in the feed, 3. Prior to all the reaction runs, the catalysts were subjected to a partial reduction in a H_2 and N_2 stream (1 h at 350 °C, 2 bar and with a flow rate of 30 cm^3_{H2} min^{-1} and 30 cm^3_{N2} min^{-1}).

2.4. Reaction indices

The conversions of CO_2 (X_{CO2}) and of CO_x (X_{COx}) were defined according to the expressions:

$$X_{CO_2} = \frac{F^0_{CO_2} - F_{CO_2}}{F^0_{CO_2}} \cdot 100 \quad (1)$$

$$X_{CO_x} = \frac{F^0_{CO_x} - F_{CO_x}}{F^0_{CO_x}} \cdot 100 \quad (2)$$

where F^0_{CO2} and F^0_{COx} are the molar flow rates of CO_2 and CO_x at the inlet of the reactor, respectively, and F_{CO2} and F_{COx} are the corresponding values at the reactor outlet stream.

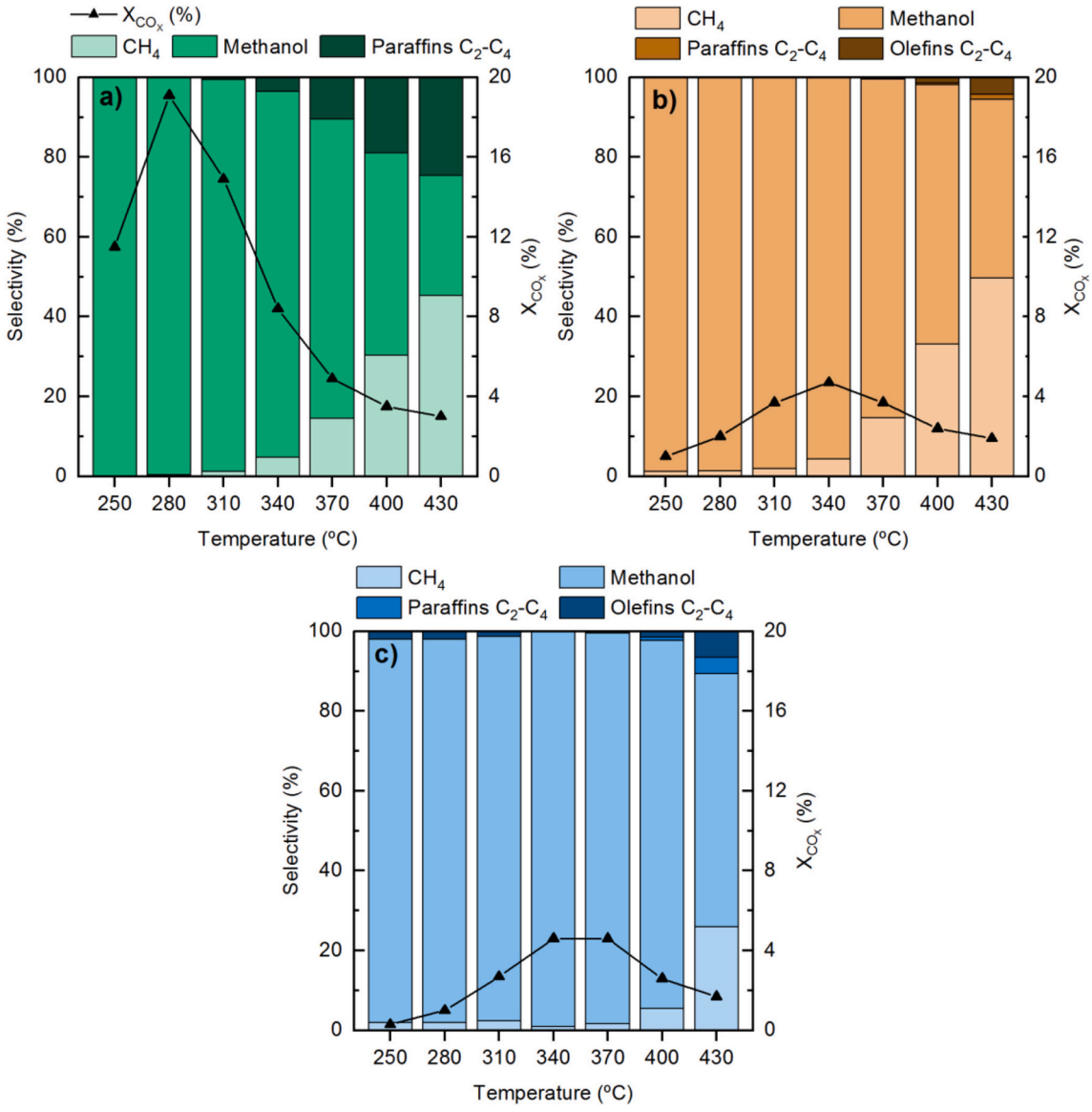

Fig. 2. Effect of temperature on CO_x conversion and selectivity of products with (a) CZZ, (b) IZ, (c) ZZ catalysts. Reaction conditions: 50 bar; 6 g_{cat} h mol_C^{-1}; CO_2/CO_x, 0.5; H_2/CO_x, 3.

The yield and selectivity of each *i* product (Y_i and S_i, respectively) excluding CO_2 and CO, were calculated as:

$$Y_i = \frac{n_i \cdot F_i}{F^0_{CO_x}} \cdot 100 \quad (3)$$

$$S_i = \frac{n_i \cdot F_i}{\sum_i (n_i \cdot F_i)} \cdot 100 \quad (4)$$

where n_i is the number of carbon atoms of the *i* compound and F_i the molar flow rate of the *i* compound in the products stream in content C atoms. It should be noted that with the definition of yields in Eq. (2), X_{COx} is the sum of the yields.

3. Results and discussion

3.1. Performance of the metallic catalysts in the methanol synthesis step

The reactions presented in this section were conducted without zeolite, with the aim of testing the metallic catalysts alone in the first stage of the gasoline production (synthesis of methanol) in the 250–430 °C range. Fig. 2 shows the effect of the temperature on the conversion (X_{COx}) of an equimolar mixture of CO_2 and CO, and on the selectivity of methanol and other byproducts (CH_4, C_2-C_4 paraffins and C_2-C_4 olefins) with the three catalysts. Comparing the results, notable differences are observed. With CZZ catalyst (Fig. 2a), high conversion was reached at low temperature. In fact, X_{COx} accounted for 19% at 280 °C, which corresponds with the thermodynamics prediction [14,66–68]. Moreover, the selectivity of oxygenates (mainly methanol, with an insignificant DME content) was 100%. Nonetheless, X_{COx} decreased steadily with increasing temperature, until declining to 3.5% at 430 °C, due to the thermodynamic limitation. In addition, selectivity of methanol also decreased at high temperature due to the favoring of CO formation by the rWGS reaction. These results are in accordance with the prediction of thermodynamic studies in the literature [14,66–68]. The presence of C_2-C_4 paraffins is explained by the hydrogenation of the light olefins formed from the conversion of oxygenates, and the presence of CH_4 over 340 °C exposes the activity of CZZ in the methanation at this temperature.

X_{COx} values were lower with the IZ (Fig. 2b) and ZZ (Fig. 2c) catalysts. These catalysts had similar activity, lower than that of the CZZ catalyst. The X_{COx} reached a maximum value of 4.7% at 340 °C with IZ catalyst, and between 340 and 370 °C with ZZ catalyst, which decreased above these temperatures due to thermodynamic limitations, that also affect to the conversion of CO [14,66,67]. It is noteworthy that methanol selectivity was higher with IZ and ZZ catalysts than with the CZZ catalyst (Fig. 2a). In this sense, the best performance corresponded to the ZZ catalyst, with a methanol selectivity of almost 100% in the 340–370 °C range. Indeed, selectivity only decreased slightly with increasing temperature up to 430 °C. Considering the aforementioned results, the higher activity of CZZ catalyst for methanol production below 300 °C (with a maximum at 280 °C) is of arguable interest from the perspective of its use in the direct conversion of CO_2/CO mixtures to hydrocarbons, since this reaction must be performed at higher temperature to achieve the extent of the dual cycle mechanism to obtain C_{5+} hydrocarbons. In this regard, the reduced methanation activity of the ZZ catalyst in the 300–400 °C is of particular interest. It is noteworthy that this better performance of the ZZ catalyst with respect to the other catalysts cannot be attributed to the properties of its porous structure (Table 1), because these are less favorable for the diffusion of the reactants and products. Consequently, it should be attributed to the high activity and selectivity of the active sites of the ZZ catalyst in the methanol formation mechanism explained by Wang et al. [41] with formate ions and CO as intermediates in the reaction pathway.

In Fig. 3 the effect of the feed composition (CO_2/CO_x ratio) on methanol yield is shown. The results correspond to 350 °C, temperature considered as limit to avoid the sintering of the Cu on CZZ catalyst [27]. This catalyst is the most active for CO hydrogenation, with a methanol yield of 21%, higher than with IZ (4%) and ZZ (2%) catalysts. At higher CO_2/CO_x ratio, methanol yield remarkably decreased with CZZ catalyst. This trend fits with previous findings regarding the effect of the CO_2 content in the feed [66,69] in high conversion conditions (high concentration of methanol), for which the presence of CO is preferable to CO_2, as it eases the H_2O removal by means of the WGS reaction. As could be expected, the methanol yield in the CO_2 conversion is lower than that obtained in the literature with catalysts of similar composition under optimal conditions for methanol synthesis, i.e., lower temperature and higher pressure than those used [70]. On the other hand, the results with IZ and ZZ catalysts showed a similar trend. They both exhibited the highest methanol yield when the carbon source of the feed was 50% CO and 50% CO_2. This concurs well with previous works in the literature with the IZ catalyst [25,56]. This occurs because the reaction mechanism lies on the creation and eradication of oxygen vacancies, and the joint feed boosts this process and, additionally, favors the preservation of the oxygen vacancies.

It is also outstanding in Fig. 3 that, for the hydrogenation of CO_2 (CO_2/CO_x of 1), the obtained methanol yield was similar with the three catalysts. This result evidences the aforementioned limitation of the equilibrium conversion, and that this conversion is low in CO_2 hydrogenation. This is in accordance with thermodynamic studies in the literature [14,66–68]. It is also observed that with IZ catalyst methanol yield was similar in CO and CO_2 hydrogenation.

3.2. Performance of the tandem catalysts in the direct synthesis of hydrocarbons

With the purpose of assessing the performance of the metallic catalysts used in tandem, in Figs. 4 and 5 corresponding to IZ/HZSM-5 and ZZ/HZSM-5, respectively, the effect of temperature (340–420 °C range) and pressure (30 and 50 bar) on the conversion of CO_x (sum of the products yields, Eq. (2)) and CO_2 and on the different products yield is shown. The results correspond in both cases to an equimolar feed of CO_2 and CO (CO_2/CO_x of 0.5) and hydrogen. It should be noted that the results for the CZZ/HZSM-5 catalyst are not shown because the sintering of Cu above 320 °C was verified. In fact, an increase of the crystal size from ~10 nm (fresh catalyst) to ~35 nm was determined by XRD analysis of the spent catalyst (Table S2). On the contrary, IZ/HZSM-5 and ZZ/HZSM-5 spent catalysts maintained constant their properties in long reaction runs at these temperatures. Consequently, the attention was focused in these two catalysts because of their stability in the required temperature range.

It is also remarkable (in Figs. 4 and 5) that the C_{5+} hydrocarbons are the main products for the two catalysts and the oxygenates are almost

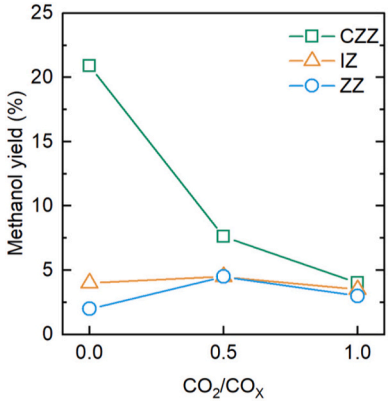

Fig. 3. Effect of the feed composition on methanol yield with CZZ, IZ and ZZ catalysts. Reaction conditions: 350 °C; 50 bar; 6 g_{cat} h mol_C^{-1}; H_2/CO_x, 3.

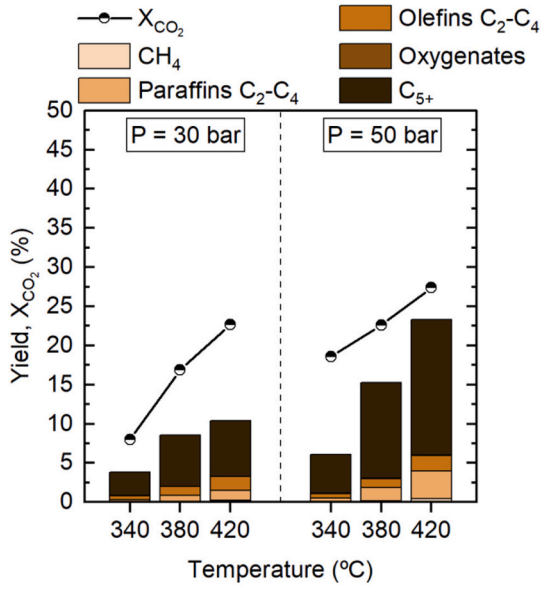

Fig. 4. Effect of temperature on CO_2 conversion, CO_x conversion (sum of the yields) and products yield at 30 and 50 bar with IZ/HZSM-5 tandem catalyst. Reaction conditions: 12 g_{cat} h mol_C^{-1}; CO_2/CO_x, 0.5; H_2/CO_x, 3.

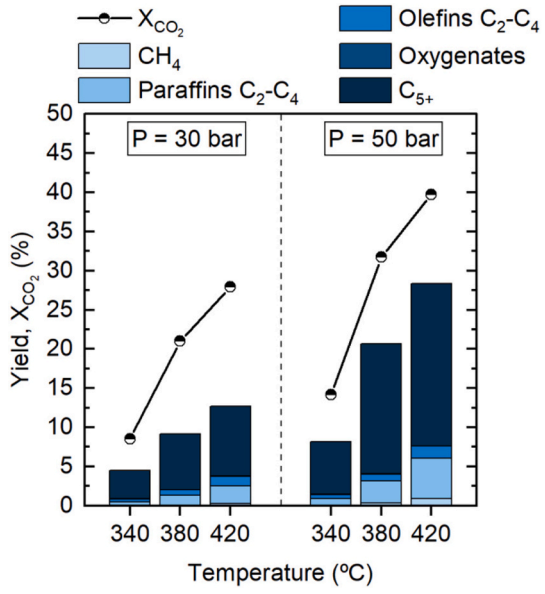

Fig. 5. Effect of temperature on CO_2 conversion, CO_x conversion (sum of the yields) and products yield at 30 and 50 bar with ZZ/HZSM-5 tandem catalyst. Reaction conditions: 12 g_{cat} h mol_C^{-1}; CO_2/CO_x, 0.5; H_2/CO_x, 3.

completely converted. At higher pressure, the results upturned, boosting the overall CO_x conversion. Regarding the IZ/HZSM-5 catalyst (Fig. 4) at 30 bar, the influence of the temperature was more subdued. CO_x conversion did not increase >2% when rising temperature from 380 to 420 °C. Regarding the CO_2 conversion, it was more affected by temperature at the lower pressure of 30 bar, rising from 8% to 23% by increasing temperature from 340 to 420 °C. For its part, at 50 bar, the CO_2 conversion reached 28% at 420 °C. At 420 °C and lower pressure (30 bar), the C_{5+} hydrocarbons yield was of approximately 7%, with a CO_x conversion of 22%. Nonetheless, under a pressure of 50 bar and at the same temperature, the obtained products were highly interesting for the insight into sustainable fuels production. With almost no methane yield (<0.5% at 30 bar), and nearly complete oxygenates conversion, the remaining products were composed of C_2-C_4 paraffins (with a yield of 3.5%), C_2-C_4 olefins (2%) and C_{5+} heavier compounds (17.3%) at the optimal conditions. The presence of olefins was not particularly outstanding, as they are chiefly hydrogenated due to the high H_2 partial pressure.

For ZZ/HZSM-5 catalyst (Fig. 5) the result of C_{5+} hydrocarbon yield was even improved compared to IZ/HZSM-5. The CO_2 conversion boosted from 8.1% to 28.3% when increasing the temperature from 340 to 420 °C (at 30 bar); and the CO_x conversion enhanced from 12.8% to 28.3% when rising the operating pressure from 30 to 50 bar (at 420 °C). In addition, the CO_2 conversion reached 40% under 420 °C and 50 bar, since, unlike IZ, ZZ catalyst hardly inhibits the rWGS reaction. Under such conditions, besides methane and methanol (whose yield did not exceed 1%), C_2-C_4 paraffins, C_2-C_4 olefins and C_{5+} hydrocarbons yields accounted for 5.1%, 1.5% and 20.7%, respectively. These hydrocarbons were mainly composed by 5 and 6 carbon number isoparaffins and some cyclic hydrocarbons that will be further itemized below.

Fig. 6 shows the CO_2 conversion and the product distribution (in yield terms) achieved with each catalyst in the optimal conditions (420 °C and 50 bar) for the hydrogenation of CO_2 and of an equimolar mixture of CO_2 and CO. There are some remarkable aspects to highlight in these results that evidence the better performance of the ZZ/HZSM-5 catalyst. As mentioned above, CZZ was not an applicable catalyst for H_2 + CO_2 valorization. At temperatures above 350 °C Cu sintered, because of both temperature and water content (especially high with CO_2 content feeds). Nevertheless, the results with this catalyst are summarized in Fig. S3. The CO_x conversion at 420 °C and 50 bar did not reach 2.5% with the CZZ/HZSM-5 catalyst, since almost no oxygenates were produced at these conditions. On the other hand, with the hybrid feed (CO_2/CO_x = 0.5) there was a higher content of oxygenates, which, however, were not successfully converted into C_{5+} hydrocarbons (<3%), as roughly all the hydrocarbons remained as C_2-C_4 paraffins, due to the poor synergy between sintered CZZ and the HZSM-5. This poor performance of CZZ is explained by the accumulation of unfavorable circumstances such as the sintering of Cu in the catalyst (Table S2) and the reduced activity of Cu catalysts for CO_2 conversion. These circumstances further deteriorate under the used reaction conditions (unfavorable for the methanol synthesis step according to thermodynamics) [14,66–68]. With regard to IZ/HZSM-5 catalyst, as noted above, it showed better performance with a mixture of CO and CO_2 in the feed, which is in agreement with the finding of Araújo et al. [56] about the better preservation of the oxygen vacancies for higher CO content in the feed than for a CO_2 and hydrogen feed. Besides the reduced conversion, the production of gasoline-range hydrocarbons fell sharply for the H_2 + CO_2 feed, revealing that IZ might not be the best metallic catalyst for gasoline-range hydrocarbon production in these operating conditions. In fact, the conversions (X_{CO2} and X_{COx}) and C_{5+} hydrocarbons yield was higher with ZZ/HZSM-5 catalyst for both feeds. The values obtained for these indices with the CO_2/CO mixture were of 39.7%, 28.4% and 20.7%, respectively. Additionally, ZZ/HZSM-5 was not affected by the higher content of CO_2 in the feed in such manner. Actually, the CO_x conversion fell merely from 28% to 26% for H_2 + CO_2 feed. All this evidences the powerful interest of the ZZ/HZSM-5 as a feasible industry catalyst, as it could cope adequately with the current fluctuations of the feed composition in this process.

In order to assess the importance of the synergy of the tandem catalysts on the reaction mechanisms, both in the synthesis of oxygenates and in the conversion of these into hydrocarbons, in Fig. 7 the effect of the temperature on the CO_x conversion for IZ and ZZ metallic catalysts and for IZ/HZSM-5 and ZZ/HZSM-5 tandem catalysts is compared. The results correspond to the hydrogenation of the equimolar mixture of CO_2 and CO. As aforementioned in the synthesis of methanol (Fig. 2), the results were similar for the two catalysts above 350 °C as a consequence of the thermodynamic constraints. These constraints are removed with the presence of the HZSM-5 zeolite in the tandem catalysts, due to the shift of the equilibrium by the immediate conversion of the oxygenates.

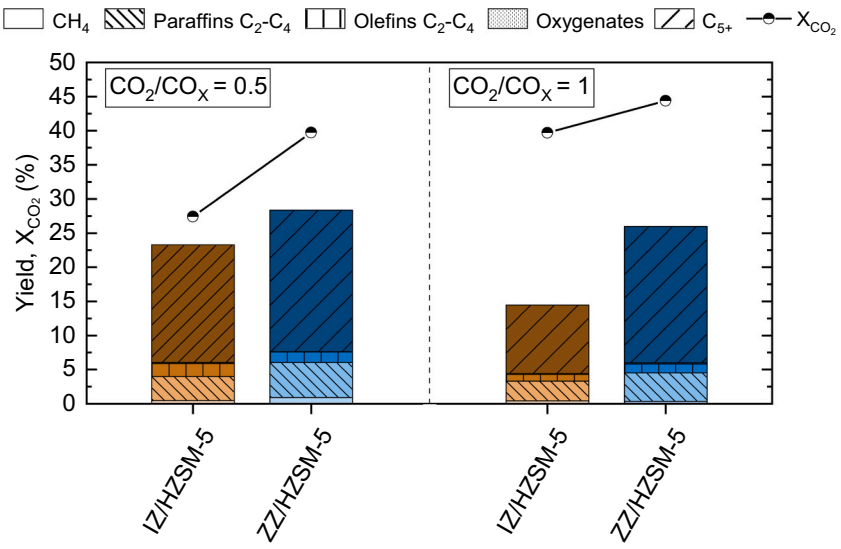

Fig. 6. Comparison of CO_2 conversion, CO_x conversion (sum of the yields) and products yield with IZ/HZSM-5 and ZZ/HZSM-5 tandem catalysts, for two different feeds. Reaction conditions: 420 °C; 50 bar; 12 g_{cat} h mol_C^{-1}; H_2/CO_x, 3.

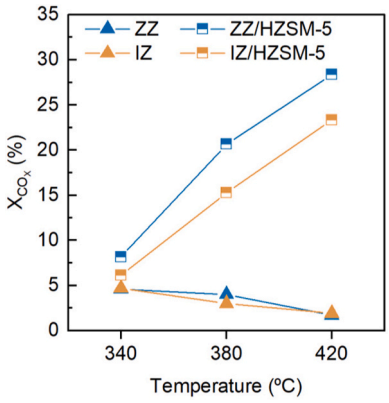

Fig. 7. Comparison of the evolution CO_x conversion with temperature in the synthesis of methanol (with IZ and ZZ catalysts) and of hydrocarbons (with IZ/HZSM-5 and ZZ/HZSM-5 catalysts). Reaction conditions: 50 bar; 12 g_{cat} h mol_C^{-1}; CO_2/CO_x, 0.5; H_2/CO_x, 3.

When comparing the results of the two tandem catalysts, the benefit of the synergy between the two reaction steps was more remarkable with the ZZ/HZSM-5 catalyst. At optimal conditions for the integrated process (420 °C and 50 bar), CO_x conversion was multiplied ~12 times (from 1.8% to 23%) with IZ/HZSM-5 with respect to the synthesis of methanol with IZ catalyst, whereas it increased a factor of >15 with the ZZ/HZSM-5 catalyst (from 1.8% to 28%) with respect to ZZ catalyst.

Fig. 8 exhibits the yield of the different hydrocarbons in the products stream with IZ/HZSM-5 (Fig. 8a) and ZZ/HZSM-5 (Fig. 8b) catalysts. These results allow to compare the performance of the two catalysts from the perspective of product interest. Additionally, the comparison of the results in the hydrogenation of the equimolar mixture of CO_2 and CO, and of CO_2 was assessed. The majority of hydrocarbons produced with both catalysts were C_6, C_5 and C_4 (in this order from highest to lowest). The highest yields (9.8%, 8.6%, and 4.1%, respectively) were obtained with ZZ/HZSM-5 catalyst for the equimolar mixture. In addition, with this catalyst the yield of C_6 fraction was virtually the same in the hydrogenation of CO_2 and of the CO_2/CO mixture, which evidences that ZZ/HZSM-5 catalyst withstands in a good way the fluctuations in the feed. It is also remarkable that the gasoline fraction (C_{5+} with a yield of 20.7% with ZZ/HZSM-5 catalyst) was mainly isoparaffinic with both catalysts. This elevated isoparaffin content is in accordance with the well-established activity of the HZSM-5 zeolite-based catalysts for the isomerization of the corresponding linear paraffins [71]. In addition, using HZSM-5 catalysts doped with Zn (by ion exchange or isomorphically substituted) in the conversion of DME at high pressure and in the presence of H_2, the high hydroisomerization activity of Zn, favored by its capacity for H_2 dissociation and surface H generation, has been determined [72,73]. Because of the favorable conditions, the total yield of C_5 and C_6 isoparaffins (2- methylbutane, 2-methylpentane and 3-methylpentane) reached nearly 20% in these operating conditions, with almost no C_{4+} n-paraffin production. Besides, the high temperature and the elevated hydrogen content hinder the dehydrocyclization and aromatization reactions, resulting in low yield of cycloalkanes (2.6%) and aromatics (0.1%). On the other hand, compounds of >7 carbon atoms were not very significant (with a total yield of 2.3%). These results are a consequence of the properties of the metallic oxide and the zeolite used in the tandem catalyst. In this way, the hydrogenating activity of the Zn-based metallic catalyst in high pressure conditions and with the presence of H_2 hindered the formation of aromatics [73]. This behavior of the Zn is different from that without the presence of H_2 in the feed, where the presence of CO_2 favors the formation of aromatics from methanol [74]. On the other hand, the moderate total acidity and the Brönsted/Lewis ratio of HZSM-5 limited the extent of heavier hydrocarbon formation reactions [74]. Consequently, the high isoparaffin content and the low presence of linear paraffins resulted in a high Research Octane Number (RON) hydrocarbon mixture with ZZ/HZSM-5 catalyst (RON of 91.8 determined according to the method proposed by Anderson, Sharkey and Walsh [75]), indicating high quality gasoline fraction. Its characteristic composition, without the presence of aromatic compounds, is of great interest for its incorporation to the refinery gasoline pool.

As concluded in preceding results in Fig. 8, comparing the catalysts, ZZ showed better performance than IZ when operating in tandem with HZSM-5. Nonetheless, for each feed composition, the trend for both catalysts was virtually the same. However, it is observed that IZ/HZSM-5 catalyst was more afflicted by alterations in feed compositions (Fig. 8a), resulting in considerably lower yield of isoparaffins with an increasing CO_2/CO_x ratio, whereas ZZ/HZSM-5 catalyst withstood better the changes in feed, maintaining almost unchanged the production of isoparaffins (Fig. 8b).

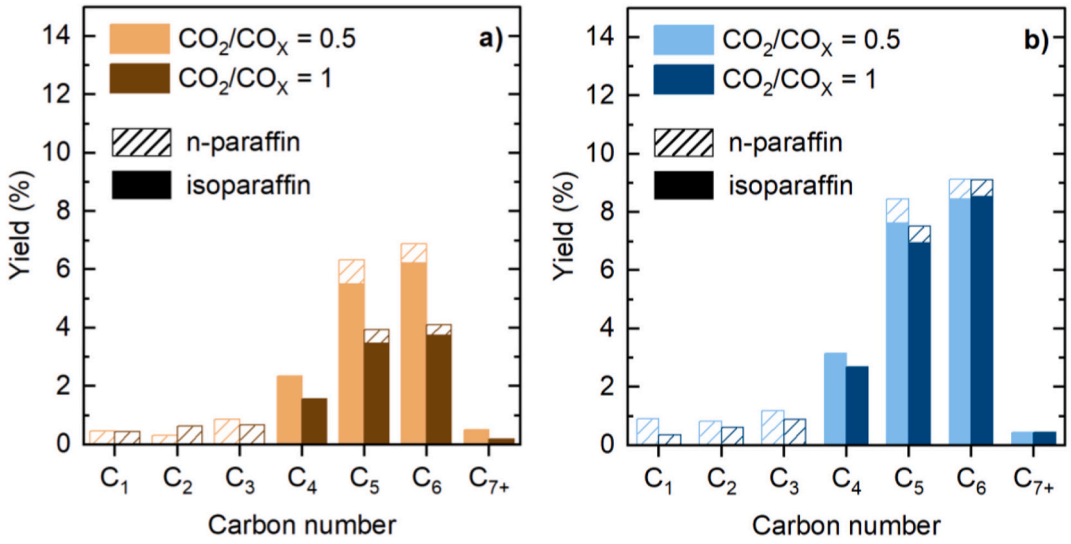

Fig. 8. Effect of the feed composition on n-paraffin and isoparaffin yield, classified by carbon number with (a) IZ/HZSM-5 and (b) ZZ/HZSM-5 tandem catalysts. Reaction conditions: 420 °C, 50 bar, 12 g_{cat} h mol_C^{-1}, $H_2/CO_x = 3$.

4. Conclusions

The results ratify the good performance (high activity, selectivity of methanol and stability) of In_2O_3-ZrO_2 and ZnO-ZrO_2 catalysts in methanol synthesis, especially from CO_2, and also from CO_2/CO mixtures, at appropriate conditions for the direct synthesis of hydrocarbons. Moreover, both catalysts showed great performance when used in tandem together with a HZSM-5 zeolite, exposing the effective synergy between the mechanisms of methanol formation and its conversion into hydrocarbons, obtaining a high yield of C_{5+} hydrocarbons.

It is especially significant the performance of ZnO-ZrO_2/HZSM-5 catalyst, with which at 420 °C, 50 bar, CO_2/CO_x of 0.5 and H_2/CO_x of 3, a yield of C_{5+} of 20.7% was obtained. Under such conditions, CO_2 and CO_x conversions were very high, of 39.7% and 28.4%, respectively. An interesting advantage of this catalyst with respect to In_2O_3-ZrO_2/HZSM-5 is the low dependence of the results to the CO_2/CO_x ratio in the feed, which provides high versatility in the operation, combining the targets of valorizing CO_2 and syngas derived from gasification of biomass or waste from the consumer society.

The good results of gasoline production with ZnO-ZrO_2/HZSM-5 catalyst from CO_2 and mixtures of CO_2/CO allow to value positively the interest of this route as a complementary route to others studied in the literature for the production of other hydrocarbons, such as light olefins, light paraffins or aromatics. The C_{5+} fraction obtained consisted mainly of C_5 and C_6 isoparaffins, with a yield of isoparaffins of 20% and 0.1% of aromatics. With a RON of 91.8, the obtained product had a very interesting composition for its incorporation into the refinery gasoline pool. Therefore, it can be combined with other streams which, like those derived from fluidized catalytic cracking (FCC), have a content of aromatics and olefins that exceeds legal limitations. In addition, the results can be considered pioneering for this purpose with this catalyst, and they provide good prospects for improvements in the catalyst and in the optimization of the reaction conditions.

CRediT authorship contribution statement

Onintze Parra: Conceptualization, Investigation, Writing – original draft, Writing – review & editing. **Ander Portillo:** Validation, Visualization, Methodology, Writing – review & editing. **Javier Ereña:** Project administration, Funding acquisition. **Andrés T. Aguayo:** Methodology, Resources, Supervision, Project administration, Funding acquisition. **Javier Bilbao:** Conceptualization, Writing – original draft, Writing – review & editing, Project administration, Funding acquisition. **Ainara Ateka:** Conceptualization, Writing – original draft, Writing – review & editing.

Declaration of Competing Interest

The authors declare that they have no known competing financial interests or personal relationships that could have appeared to influence the work reported in this paper.

Data availability

The authors are unable or have chosen not to specify which data has been used.

Acknowledgements

This work has been carried out with the financial support of the Ministry of Science, Innovation and Universities of the Spanish Government (PID2019-108448RB-100); the Basque Government (Project IT1645-22), the European Regional Development Funds (ERDF) and the European Commission (HORIZON H2020-MSCA RISE-2018. Contract No. 823745). O. Parra is grateful for the financial support of the grant of the Basque Government (PRE_2021_1_0014) and A. Portillo is grateful for the grant from the Ministry of Science, Innovation and Universities of the Spanish Government (BES2017-081135). The authors thank for technical and human support provided by SGIker (UPV/EHU).

Appendix A. Supplementary data

Supplementary data to this article can be found online at https://doi.org/10.1016/j.fuproc.2023.107745.

References

[1] W. Zhou, K. Cheng, J. Kang, C. Zhou, V. Subramanian, Q. Zhang, Y. Wang, New horizon in C1 chemistry: breaking the selectivity limitation in transformation of syngas and hydrogenation of CO_2 into hydrocarbon chemicals and fuels, Chem. Soc. Rev. 48 (2019) 3193–3228, https://doi.org/10.1039/c8cs00502h.

[2] E.C. Ra, K.Y. Kim, E.H. Kim, H. Lee, K. An, J.S. Lee, Recycling carbon dioxide through catalytic hydrogenation: recent key developments and perspectives, ACS Catal. 10 (2020) 11318–11345, https://doi.org/10.1021/ACSCATAL.0C02930.

[3] S. Saeidi, S. Najari, V. Hessel, K. Wilson, F.J. Keil, P. Concepción, S.L. Suib, A. E. Rodrigues, Recent advances in CO_2 hydrogenation to value-added products —

current challenges and future directions, Prog. Energy Combust. Sci. 85 (2021), 100905, https://doi.org/10.1016/j.pecs.2021.100905.
[4] Z. Zhou, P. Gao, Direct carbon dioxide hydrogenation to produce bulk chemicals and liquid fuels via heterogeneous catalysis, Chin. J. Catal. 43 (2022) 2045–2056, https://doi.org/10.1016/S1872-2067(22)64107-X.
[5] E. Yoo, U. Lee, G. Zang, P. Sun, A. Elgowainy, M. Wang, Incremental approach for the life-cycle greenhouse gas analysis of carbon capture and utilization, J. CO2 Util. 65 (2022) 102212, https://doi.org/10.1016/J.JCOU.2022.102212.
[6] S. De, A. Dokania, A. Ramirez, J. Gascon, Advances in the design of heterogeneous catalysts and thermocatalytic processes for CO_2 utilization, ACS Catal. 10 (2020) 14147–14185, https://doi.org/10.1021/ACSCATAL.0C04273.
[7] T.A. Atsbha, T. Yoon, P. Seongho, C.J. Lee, A review on the catalytic conversion of CO_2 using H_2 for synthesis of CO, methanol, and hydrocarbons, J. CO2 Util. 44 (2021) 101413, https://doi.org/10.1016/j.jcou.2020.101413.
[8] Y. Gambo, S. Adamu, R.A. Lucky, M.S. Ba-Shammakh, M.M. Hossain, Tandem catalysis: a sustainable alternative for direct hydrogenation of CO_2 to light olefins, Appl. Catal. A Gen. 641 (2022), 118658, https://doi.org/10.1016/j.apcata.2022.118658.
[9] H. Wang, S. Fan, S. Wang, M. Dong, Z.F. Qin, W. Bin Fan, J.G. Wang, Research progresses in the hydrogenation of carbon dioxide to certain hydrocarbon products, Ranliao Huaxue Xuebao/Journal Fuel Chem. Technol. 49 (2021) 1609–1619, https://doi.org/10.1016/S1872-5813(21)60122-6.
[10] B. Pawelec, R. Guil-López, N. Mota, J.L.G. Fierro, R.M. Navarro Yerga, Catalysts for the conversion of CO_2 to low molecular weight olefins—a review, Materials (Basel) 14 (2021) 6952, https://doi.org/10.3390/ma14226952.
[11] A. Ramirez, X. Gong, M. Caglayan, S.A.F. Nastase, E. Abou-Hamad, L. Gevers, L. Cavallo, A. Dutta Chowdhury, J. Gascon, Selectivity descriptors for the direct hydrogenation of CO_2 to hydrocarbons during zeolite-mediated bifunctional catalysis, Nat. Commun. 121 (12) (2021) 1–13, https://doi.org/10.1038/s41467-021-26090-5.
[12] P. Sharma, J. Sebastian, S. Ghosh, D. Creaser, L. Olsson, Recent advances in hydrogenation of CO_2 into hydrocarbons via methanol intermediate over heterogeneous catalysts, Catal, Sci. Technol. 11 (2021) 1665–1697, https://doi.org/10.1039/d0cy01913e.
[13] S. Ghosh, L. Olsson, D. Creaser, Methanol mediated direct CO_2 hydrogenation to hydrocarbons: Experimental and kinetic modeling study, Chem. Eng. J. 435 (2022), 135090, https://doi.org/10.1016/j.cej.2022.135090.
[14] S. Guo, H. Wang, Z. Qin, Z. Li, G. Wang, M. Dong, W. Fan, J. Wang, Feasibility, limit, and suitable reaction conditions for the production of alcohols and hydrocarbons from CO and CO_2 through hydrogenation, a thermodynamic consideration, Ind. Eng. Chem. Res. 61 (2022) 17027–17038, https://doi.org/10.1021/acs.iecr.2c02898.
[15] X. Jiang, X. Nie, X. Guo, C. Song, J.G. Chen, Recent advances in carbon dioxide hydrogenation to methanol via heterogeneous catalysis, Chem. Rev. 120 (2020) 7984–8034, https://doi.org/10.1021/ACS.CHEMREV.9B00723/.
[16] M. Heenemann, M.M. Millet, F. Girgsdies, M. Eichelbaum, T. Risse, R. Schlögl, T. Jones, E. Frei, The mechanism of interfacial CO2 activation on Al doped Cu/ZnO, ACS Catal. 10 (2020) 5672–5680, https://doi.org/10.1021/ACSCATAL.0C00574.
[17] Y. Wang, X. Wang, Z. Yan, C. Xu, W. Zhang, H. Ban, C. Li, Activation reconstructing CuZnO/SiO_2 catalyst for CO_2 hydrogenation, J. Catal. 412 (2022) 10–20, https://doi.org/10.1016/j.jcat.2022.06.003.
[18] R. Dalebout, L. Barberis, G. Totarella, S.J. Turner, C. La Fontaine, F.M.F. de Groot, X. Carrier, A.M.J. van der Eerden, F. Meirer, P.E. de Jongh, Insight into the nature of the ZnO_X promoter during methanol synthesis, ACS Catal. 12 (2022) 6628, https://doi.org/10.1021/ACSCATAL.1C05101.
[19] M. Behrens, G. Lolli, N. Muratova, I. Kasatkin, M. Hävecker, R.N. d'Alnoncourt, O. Storcheva, K. Köhler, M. Muhler, R. Schlögl, The effect of Al-doping on ZnO nanoparticles applied as catalyst support, Phys. Chem. Chem. Phys. 15 (2013) 1374–1381, https://doi.org/10.1039/C2CP41680H.
[20] M. Sánchez-Contador, A. Ateka, P. Rodriguez-Vega, J. Bilbao, A.T. Aguayo, Optimization of the Zr content in the CuO-ZnO-ZrO_2/SAPO-11 catalyst for the selective hydrogenation of CO+CO_2 mixtures in the direct synthesis of dimethyl ether, Ind. Eng. Chem. Res. 57 (2018) 1169–1178, https://doi.org/10.1021/acs.iecr.7b04345.
[21] Y. Zhang, J. Fei, Y. Yu, X. Zheng, Methanol synthesis from CO_2 hydrogenation over Cu based catalyst supported on zirconia modified γ-Al_2O_3, Energy Convers. Manag. 47 (2006) 3360–3367, https://doi.org/10.1016/J.ENCONMAN.2006.01.010.
[22] Y. Yang, J. Evans, J.A. Rodriguez, M.G. White, P. Liu, Fundamental studies of methanol synthesis from CO_2 hydrogenation on Cu(111), Cu clusters, and Cu/ZnO (000), Phys. Chem. Chem. Phys. 12 (2010) 9909–9917, https://doi.org/10.1039/C001484B.
[23] L.C. Grabow, M. Mavrikakis, Mechanism of methanol synthesis on cu through CO2 and CO hydrogenation, ACS Catal. 1 (2011) 365–384, https://doi.org/10.1021/CS200055D.
[24] T. Reichenbach, K. Mondal, M. Jäger, T. Vent-Schmidt, D. Himmel, V. Dybbert, A. Bruix, I. Krossing, M. Walter, M. Moseler, Ab initio study of CO_2 hydrogenation mechanisms on inverse ZnO/Cu catalysts, J. Catal. 360 (2018) 168–174, https://doi.org/10.1016/j.jcat.2018.01.035.
[25] O. Martin, A.J. Martín, C. Mondelli, S. Mitchell, T.F. Segawa, R. Hauert, C. Drouilly, D. Curulla-Ferré, J. Pérez-Ramírez, Indium oxide as a superior catalyst for methanol synthesis by CO_2 hydrogenation, Angew. Chem. Int. Ed. 55 (2016) 6261–6265, https://doi.org/10.1002/ANIE.201600943.
[26] X.Y. Meng, C. Peng, J. Jia, P. Liu, Y.L. Men, Y.X. Pan, Recent progress and understanding on In_2O_3-based composite catalysts for boosting CO_2 hydrogenation, J. CO2 Util. 55 (2022) 101844, https://doi.org/10.1016/j.jcou.2021.101844.
[27] A. Ateka, P. Rodriguez-Vega, J. Ereña, A.T. Aguayo, J. Bilbao, A review on the valorization of CO_2. Focusing on the thermodynamics and catalyst design studies of the direct synthesis of dimethyl ether, Fuel Process. Technol. 233 (2022) 107310, https://doi.org/10.1016/J.FUPROC.2022.107310.
[28] M.S. Frei, M. Capdevila-Cortada, R. García-Muelas, C. Mondelli, N. López, J. A. Stewart, D. Curulla Ferré, J. Pérez-Ramírez, Mechanism and microkinetics of methanol synthesis via CO_2 hydrogenation on indium oxide, J. Catal. 361 (2018) 313–321, https://doi.org/10.1016/j.jcat.2018.03.014.
[29] A. Posada-Borbón, H. Grönbeck, A first-principles-based microkinetic study of CO_2 reduction to CH_3OH over In_2O_3(110), ACS Catal. 11 (2021) 9996–10006, https://doi.org/10.1021/ACSCATAL.1C01707.
[30] A. Portillo, A. Ateka, J. Ereña, J. Bilbao, A.T. Aguayo, Role of Zr loading into In_2O_3 catalysts for the direct conversion of CO_2/CO mixtures into light olefins, J. Environ. Manag. 316 (2022), 115329, https://doi.org/10.1016/j.jenvman.2022.115329.
[31] J. Wang, G. Zhang, J. Zhu, X. Zhang, F. Ding, A. Zhang, X. Guo, C. Song, CO_2 hydrogenation to methanol over In_2O_3-based catalysts: from mechanism to catalyst development, ACS Catal. 11 (2021) 1406–1423, https://doi.org/10.1021/acscatal.0c03665.
[32] J. Zhu, F. Cannizzaro, L. Liu, H. Zhang, N. Kosinov, I.A.W. Filot, J. Rabeah, A. Brückner, E.J.M. Hensen, Ni-in synergy in CO_2 hydrogenation to methanol, ACS Catal. 11 (2021) 11371–11384, https://doi.org/10.1021/acscatal.1c03170.
[33] N. Rui, Z. Wang, K. Sun, J. Ye, Q. Ge, C. Jun Liu, CO_2 hydrogenation to methanol over Pd/In_2O_3: effects of Pd and oxygen vacancy, Appl. Catal. B Environ. 218 (2017) 488–497, https://doi.org/10.1016/J.APCATB.2017.06.069.
[34] G. Tian, Y. Wu, S. Wu, S. Huang, J. Gao, CO_2 hydrogenation to methanol over Pd/MnO/In_2O_3 catalyst, J. Environ. Chem. Eng. 10 (2022), https://doi.org/10.1016/J.JECE.2021.106965.
[35] J. Wang, K. Sun, X. Jia, C. Jun Liu, CO_2 hydrogenation to methanol over Rh/In_2O_3 catalyst, Catal. Today 365 (2021) 341–347, https://doi.org/10.1016/J.CATTOD.2020.05.020.
[36] Z. Han, C. Tang, J. Wang, L. Li, C. Li, Atomically dispersed Ptn+ species as highly active sites in Pt/In_2O_3 catalysts for methanol synthesis from CO_2 hydrogenation, J. Catal. 394 (2021) 236–244, https://doi.org/10.1016/j.jcat.2020.06.018.
[37] N. Rui, F. Zhang, K. Sun, Z. Liu, W. Xu, E. Stavitski, S.D. Senanayake, J. A. Rodriguez, C.J. Liu, Hydrogenation of CO_2 to methanol on a $Au^{\delta+}$-In_2O_{3-x} catalyst, ACS Catal. 10 (2020) 11307–11317, https://doi.org/10.1021/acscatal.0c02120.
[38] J. Ding, Z. Li, W. Xiong, Y. Zhang, A. Ye, W. Huang, Structural evolution and catalytic performance in CO_2 hydrogenation reaction of ZnO-ZrO_2 composite oxides, Appl. Surf. Sci. 587 (2022), 152884, https://doi.org/10.1016/j.apsusc.2022.152884.
[39] P. Šot, G. Noh, I.C. Weber, S.E. Pratsinis, C. Copéret, The influence of ZnO−ZrO_2 interface in hydrogenation of CO_2 to CH_3OH, Helv. Chim. Acta. 105 (2022), https://doi.org/10.1002/hlca.202200007.
[40] K. Lee, U. Anjum, T.P. Araújo, C. Mondelli, Q. He, S. Furukawa, J. Pérez-Ramírez, S.M. Kozlov, N. Yan, Atomic Pd-promoted $ZnZrO_x$ solid solution catalyst for CO_2 hydrogenation to methanol, Appl. Catal. B Environ. 304 (2022), 120994, https://doi.org/10.1016/j.apcatb.2021.120994.
[41] J. Wang, G. Li, Z. Li, C. Tang, Z. Feng, H. An, H. Liu, T. Liu, C. Li, A highly selective and stable ZnO-ZrO_2 solid solution catalyst for CO_2 hydrogenation to methanol, Sci. Adv. 3 (2017), https://doi.org/10.1126/sciadv.1701290.
[42] A. Portillo, A. Ateka, J. Ereña, J. Bilbao, A.T. Aguayo, Alternative acid catalysts for the stable and selective direct conversion of CO_2/CO mixtures into light olefins, Fuel Process. Technol. 238 (2022), 107513, https://doi.org/10.1016/J.FUPROC.2022.107513.
[43] M. Bjørgen, S. Svelle, F. Joensen, J. Nerlov, S. Kolboe, F. Bonino, L. Palumbo, S. Bordiga, U. Olsbye, Conversion of methanol to hydrocarbons over zeolite H-ZSM-5: on the origin of the olefinic species, J. Catal. 249 (2007) 195–207, https://doi.org/10.1016/J.JCAT.2007.04.006.
[44] S. Ilias, A. Bhan, Mechanism of the catalytic conversion of methanol to hydrocarbons, ACS Catal. 3 (2013) 18–31, https://doi.org/10.1021/CS3006583.
[45] X. Liu, M. Wang, H. Yin, J. Hu, K. Cheng, J. Kang, Q. Zhang, Y. Wang, Tandem catalysis for hydrogenation of CO and CO_2 to lower olefins with bifunctional catalysts composed of spinel oxide and SAPO-34, ACS Catal. 10 (2020) 8303–8314, https://doi.org/10.1021/ACSCATAL.0C01579.
[46] A. Portillo, A. Ateka, J. Ereña, A.T. Aguayo, J. Bilbao, Conditions for the joint conversion of CO_2 and syngas in the direct synthesis of light olefins using In_2O_3-ZrO_2/SAPO-34 catalyst, Ind. Eng. Chem. Res. 61 (2022) 10365–10376, https://doi.org/10.1021/acs.iecr.1c03556.
[47] P. Tian, G. Zhan, J. Tian, K.B. Tan, M. Guo, Y. Han, T. Fu, J. Huang, Q. Li, Direct CO_2 hydrogenation to light olefins over $ZnZrO_x$ mixed with hierarchically hollow SAPO-34 with rice husk as green silicon source and template, Appl. Catal. B Environ. 315 (2022), 121572, https://doi.org/10.1016/J.APCATB.2022.121572.
[48] W. Zhang, S. Wang, S. Guo, Z. Qin, M. Dong, W. Fan, J. Wang, Ga_mCrO_x/H-SAPO-34(F), a highly efficient bifunctional catalyst for the direct conversion of CO_2 into ethene and propene, Fuel. 329 (2022), 125475, https://doi.org/10.1016/j.fuel.2022.125475.
[49] X. Zhao, J. Li, P. Tian, L. Wang, X. Li, S. Lin, X. Guo, Z. Liu, Achieving a superlong lifetime in the zeolite-catalyzed MTO reaction under high pressure: synergistic effect of hydrogen and water, ACS Catal. 9 (2019) 3017–3025, https://doi.org/10.1021/acscatal.8b04402.
[50] P. Ticali, D. Salusso, R. Ahmad, C. Ahoba-Sam, A. Ramirez, G. Shterk, K. A. Lomachenko, E. Borfecchia, S. Morandi, L. Cavallo, J. Gascon, S. Bordiga, U. Olsbye, CO_2 hydrogenation to methanol and hydrocarbons over bifunctional Zn-

doped ZrO_2/zeolite catalysts, Catal Sci. Technol. 11 (2021) 1249–1268, https://doi.org/10.1039/D0CY01550D.
[51] R. Gao, L. Zhang, L. Wang, C. Zhang, K.W. Jun, S.K. Kim, H.G. Park, Y. Gao, Y. Zhu, H. Wan, G. Guan, T. Zhao, Efficient production of renewable hydrocarbon fuels using waste CO_2 and green H_2 by integrating Fe-based Fischer-Tropsch synthesis and olefin oligomerization, Energy. 248 (2022), 123616, https://doi.org/10.1016/j.energy.2022.123616.
[52] H. Li, C. Li, P. Guo, P. Dong, N. Xi, D. Ji, X. Zhao, Y. Zhao, G. Li, Effect of gadolinium introduced HZSM-5 zeolite on the products distribution of MTH reaction, Catal. Lett. 151 (2021) 2019–2026, https://doi.org/10.1007/S10562-020-03460-0.
[53] S. Lin, Y. Zhi, W. Chen, H. Li, W. Zhang, C. Lou, X. Wu, S. Zeng, S. Xu, J. Xiao, A. Zheng, Y. Wei, Z. Liu, Molecular routes of dynamic autocatalysis for methanol-to-hydrocarbons reaction, J. Am. Chem. Soc. 143 (2021) 12038–12052, https://doi.org/10.1021/JACS.1C03475.
[54] I. Pinilla-Herrero, E. Borfecchia, T. Cordero-Lanzac, U.V. Mentzel, F. Joensen, K. A. Lomachenko, S. Bordiga, U. Olsbye, P. Beato, S. Svelle, Finding the active species: the conversion of methanol to aromatics over Zn-ZSM-5/alumina shaped catalysts, J. Catal. 394 (2021) 416–428, https://doi.org/10.1016/J.JCAT.2020.10.024.
[55] M. Ibáñez, P. Pérez-Uriarte, M. Sánchez-Contador, T. Cordero-Lanzac, A.T. Aguayo, J. Bilbao, P. Castaño, Nature and location of carbonaceous species in a composite HZSM-5 zeolite catalyst during the conversion of dimethyl ether into light olefins, Catalysts. 7 (2017) 254, https://doi.org/10.3390/catal7090254.
[56] T.P. Araújo, A. Shah, C. Mondelli, J.A. Stewart, D. Curulla Ferré, J. Pérez-Ramírez, Impact of hybrid CO_2-CO feeds on methanol synthesis over In_2O_3-based catalysts, Appl. Catal. B Environ. 285 (2021) 119878, https://doi.org/10.1016/j.apcatb.2021.119878.
[57] A. Akbarian, A. Andooz, E. Kowsari, S. Ramakrishna, S. Asgari, Z.A. Cheshmeh, Challenges and opportunities of lignocellulosic biomass gasification in the path of circular bioeconomy, Bioresour. Technol. 362 (2022), https://doi.org/10.1016/j.biortech.2022.127774.
[58] A. Larsson, M. Kuba, T. Berdugo Vilches, M. Seemann, H. Hofbauer, H. Thunman, Steam gasification of biomass – typical gas quality and operational strategies derived from industrial-scale plants, Fuel Process. Technol. 212 (2021) 106609, https://doi.org/10.1016/j.fuproc.2020.106609.
[59] G. Lopez, M. Artetxe, M. Amutio, J. Alvarez, J. Bilbao, M. Olazar, Recent advances in the gasification of waste plastics. A critical overview, Renew. Sust. Energ. Rev. 82 (2018) 576–596, https://doi.org/10.1016/J.RSER.2017.09.032.
[60] R. Xu, C. Yan, Q. Liu, E. Liu, H. Zhang, X. Zhang, X. Yuan, L. Han, H. Lei, R. Ruan, X. Zhang, Development of metal-doping mesoporous biochar catalyst for co-valorizing biomass and plastic waste into valuable hydrocarbons, syngas, and carbons, Fuel Process. Technol. 227 (2022), 107127, https://doi.org/10.1016/j.fuproc.2021.107127.
[61] L. Tan, P. Zhang, Y. Cui, Y. Suzuki, H. Li, L. Guo, G. Yang, N. Tsubaki, Direct CO_2 hydrogenation to light olefins by suppressing CO by-product formation, Fuel Process. Technol. 196 (2019), 106174, https://doi.org/10.1016/J.FUPROC.2019.106174.
[62] Z. Li, Y. Qu, J. Wang, H. Liu, M. Li, S. Miao, C. Li, Highly selective conversion of carbon dioxide to aromatics over tandem catalysts, Joule. 3 (2019) 570–583, https://doi.org/10.1016/j.joule.2018.10.027.
[63] P.L. Benito, A.T. Aguayo, A.G. Gayubo, J. Bilbao, Catalyst equilibration for transformation of methanol into hydrocarbons by reaction-regeneration cycles, Ind. Eng. Chem. Res. 35 (1996) 2177–2182, https://doi.org/10.1021/ie950493u.
[64] M.S. Frei, C. Mondelli, A. Cesarini, F. Krumeich, R. Hauert, J.A. Stewart, D. Curulla Ferré, J. Pérez-Ramírez, Role of zirconia in indium oxide-catalyzed CO_2 hydrogenation to methanol, ACS Catal. 10 (2020) 1133–1145, https://doi.org/10.1021/ACSCATAL.9B03305.
[65] Z. Han, F. Zhou, J. Zhao, Y. Liu, H. Ma, G. Wu, Synthesis of hierarchical GaZSM-5 zeolites by a post-treatment method and their catalytic conversion of methanol to olefins, Microporous Mesoporous Mater. 302 (2020), 110194, https://doi.org/10.1016/j.micromeso.2020.110194.
[66] A. Ateka, J. Ereña, P. Pérez-Uriarte, A.T. Aguayo, J. Bilbao, Effect of the content of CO_2 and H_2 in the feed on the conversion of CO_2 in the direct synthesis of dimethyl ether over a CuO–ZnO–Al_2O_3/SAPO-18 catalyst, Int. J. Hydrog. Energy 42 (2017) 27130–27138, https://doi.org/10.1016/j.ijhydene.2017.09.104.
[67] S. Zhang, Z. Wu, X. Liu, K. Hua, Z. Shao, B. Wei, C. Huang, H. Wang, Y. Sun, A short review of recent advances in direct CO_2 hydrogenation to alcohols, Top. Catal. 64 (2021) 371–394, https://doi.org/10.1007/s11244-020-01405-w.
[68] K. Ahmad, S. Upadhyayula, Greenhouse gas CO_2 hydrogenation to fuels: a thermodynamic analysis, Environ. Prog. Sustain. Energy 38 (2019) 98–111, https://doi.org/10.1002/EP.13028.
[69] N.D. Nielsen, A.D. Jensen, J.M. Christensen, The roles of CO and CO_2 in high pressure methanol synthesis over Cu-based catalysts, J. Catal. 393 (2021) 324–334, https://doi.org/10.1016/J.JCAT.2020.11.035.
[70] Y. Xu, Z. Gao, L. Peng, K. Liu, Y. Yang, R. Qiu, S. Yang, C. Wu, J. Jiang, Y. Wang, W. Tan, H. Wang, J. Li, A highly efficient Cu_x/ZnO/ZrO_2 catalyst for selective CO_2 hydrogenation to methanol, J. Catal. 414 (2022) 236–244, https://doi.org/10.1016/j.jcat.2022.09.011.
[71] Z. Wen, C. Wang, J. Wei, J. Sun, L. Guo, Q. Ge, H. Xu, Isoparaffin-rich gasoline synthesis from DME over Ni-modified HZSM-5, Catal Sci. Technol. 6 (2016) 8089–8097, https://doi.org/10.1039/C6CY01818A.
[72] X. Su, K. Zhang, Y. Snatenkova, Z. Matieva, X. Bai, N. Kolesnichenko, W. Wu, High-efficiency nano [Zn,Al]ZSM-5 bifunctional catalysts for dimethyl ether conversion to isoparaffin-rich gasoline, Fuel Process. Technol. 198 (2020), 106242, https://doi.org/10.1016/J.FUPROC.2019.106242.
[73] L.N. Vosmerikova, Z.M. Matieva, Y.M. Snatenkova, N.V. Kolesnichenko, V. I. Zaikovskii, A.V. Vosmerikov, Conversion of dimethyl ether to liquid hydrocarbons over Zn-isomorphously substituted HZSM-5, Fuel. 320 (2022), 123959, https://doi.org/10.1016/J.FUEL.2022.123959.
[74] R. Jin, K. Ma, Z. Chen, Z. Tang, H. Hu, J. Wang, Z. Zhang, C. Dai, X. Ma, Effect of CO_2 on the catalytic performance of Zn/ZSM-5 towards the conversion of methanol to aromatics, Fuel. 332 (2023), 126247, https://doi.org/10.1016/J.FUEL.2022.126247.
[75] P.C. Anderson, J.M. Sharkey, R.P. Walsh, Calculation of research octane Number of motor gasolines from chromatographic data and a new approach to motor gasoline quality control, J. Inst. Pet. 59 (1972) 83.